Cross-equatorial northerly surges associated with extratropical cold surges and tropical variability over the Maritime Continent

Tri W. Hadi[a], Muhammad Rais Abdillah[a,*], Narizka N. Purwadani[b], Rusmawan Suwarman[a], Nurjanna Joko Trilaksono[a], Faiz R. Fajary[a,c], Madam T. Maulana[d], Dudy D. Wijaya[e]

[a]*Atmospheric Science Research Group, Faculty of Earth Sciences and Technology, Institut Teknologi Bandung, Bandung, Indonesia*

[b]*Graduate Program in Earth Science, Faculty of Earth Sciences and Technology, Institut Teknologi Bandung, Bandung, Indonesia*

[c]*Transdisciplinary Science and Engineering Program, Graduate School of Advanced Science and Engineering, Hiroshima University, Hiroshima, Japan*

[d]*Department of Geophysics, Graduate School of Science, Tohoku University, Sendai, Japan*

[e]*Geodetic Science, Engineering, and Innovation Research Group, Faculty of Earth Sciences and Technology, Institut Teknologi Bandung, Bandung, Indonesia*

**Corresponding author*: Muhammad Rais Abdillah, m.rais@itb.ac.id

Note that, this manuscript has been submitted for publication in the Journal of Climate. Although it has undergone peer review, it has not yet been accepted for publication. Subsequent versions may contain slight content revisions. If accepted, the final version will be accessible via the 'Peer-reviewed Publication DOI' link on this webpage. Please feel free to contact the authors with any comments or questions.

ABSTRACT

Cross-equatorial northerly surge (CENS) is characterized by a strengthening of northerly moist monsoon winds over south of the South China Sea in the western Maritime Continent. The CENS typically lasts a few days in boreal winter and is frequently reported as a crucial synoptic forcing of heavy rainfall and flood events over northern Java Island. The occurrence of CENS has been generally understood as an extension of northerly cold surge (CS) coming from East Asia. However, out of 117 CENS events identified over the last 42 years, only 59% of the events were induced by cold surges (CENS-CS). We further found that CENS occurred with no association to cold surges (CENS-noCS) are mostly attributed to several tropical variabilities (Madden-Julian Oscillation phases 4-7, mixed-Rossby gravity waves, equatorial Rossby waves, and tropical cyclones). These phenomena induce strengthening of northerly winds mainly by generating meridional southward pressure gradient force over the CENS region. In terms of potential impacts, precipitation anomalies over northern Java Island associated with CENS-CS are slightly larger than those of CENS-noCS but significant flood events had occurred following any CENS. These imply that both types of CENS are important for controlling hydrometeorological events over the region of interest.

SIGNIFICANCE STATEMENT

Day-to-day variation during the rainy season in the south of Indonesia is modulated by incoming northerly moist flow called cross-equatorial northerly surge (CENS) events. These events often cause heavy rain and flooding in the most densely populated island of Java, especially in Jakarta. Understanding CENS dynamics is crucial for reliable weather monitoring and forecasting systems. However, the current knowledge of CENS initiation, which is controlled by extratropical cold surge, only explains 59% of CENS events. To improve the predictability of CENS, this study identifies other potential drivers that manifest as several tropical phenomena, which provide favorable conditions for CENS events. Furthermore, we confirm that floods can occur during any CENS event, suggesting that forecasters should pay attention to all CENS regardless of their origin.

1. Introduction

A cross-equatorial northerly surge (CENS[1]) event is characterized by a strengthening in northerly sea surface wind that typically lasts few days during boreal winter in the western Maritime Continent, predominantly south of the equator between Sumatra and Borneo Islands (Hattori et al. 2011; Maulana et al. 2023). The surge intensifies northerly moist monsoon wind coming from the South China Sea and modulates rainy season variability in southern Indonesia and northern Australia (Suppiah and Wu 1998). Most of major flood events in big cities in northern Java Island, including the megapolitan city of Jakarta, were reported to be initiated by CENS events (Wu et al. 2007; Trilaksono et al. 2012; Wu et al. 2013; Siswanto et al. 2015; Hermawan et al. 2022; Lubis et al. 2022). Hence, the national meteorological agency of Indonesia (BMKG) pays special attention to CENS activity (BMKG 2024).

The occurrences of CENS are usually attributed to East Asian cold surges (CS) (Wu et al. 2007; Xavier et al. 2020), which are closely linked to amplification of Siberian High and cold air outbreaks in midlatitudes (Compo et al. 1999; Shoji et al. 2014; Abdillah et al. 2017, 2018). The outflow of CS is typically cold and dry but it gains moisture and increases surface heat fluxes once it passes low latitude seas (Abdillah et al. 2021). Southward propagation of anomalous high pressure from inland Asia to the southern South China Sea is then suggested to be a key factor in the development of a CENS event. Consequently, forecasters usually predict CENS by monitoring CS activity. However, a climatological study by Hattori et al. (2011) identified that approximately half of CENS events were not associated with CS. In addition, midlatitude CS events have several downstream pathways (Abdillah et al. 2021; Liu et al. 2021); only 39% of the events showed clear propagation to the South China Sea (Abdillah et al. 2021). Moreover, the intrusion of CS can also interact with atmospheric disturbances along its pathway such as Borneo vortex (Chang et al. 2005a; Koseki et al. 2014; Chen et al. 2015; Narulita et al. 2023) and, in such condition, the southward

[1] Other studies sometimes use another abbreviation: “CES” or cross-equatorial surge. The current study uses “CENS” to distinguish with the use of CES on southerly cross-equatorial flows occurring in boreal summer (e.g., Zhao et al. 2023)

propagation of CS is consequently diminished before reaching the Southern Hemisphere. Therefore, only some CS events actually develop into CENS, suggesting that relying on CS for CENS prediction can sometimes be problematic.

The question we are raising here is: what drives the CENS besides the extratropical CS? If CS is the only major meridionally propagating disturbance related to CENS, then the other forcings of CENS are likely to be zonally propagating tropical phenomena. One potential driver is the Madden-Julian Oscillation (MJO) (Madden and Julian 1971; Zhang 2005). As one of the main sources of tropical convective variability (Wheeler and Kiladis 1999; Kiladis et al. 2005; Fajary et al. 2019), MJO greatly affects circulation both in the tropics and extratropics (Wheeler and Hendon 2004; Stan et al. 2017). Moreover, Hattori et al. (2011) documented that some CENS events, which were unrelated to CS, were associated with MJO. However, they only considered a specific phase of MJO, and the mechanism through which the MJO drives the CENS remains unclear. Besides, about a quarter of total CENS events identified in Hattori et al. (2011) were neither associated with CS nor MJO. Hence, we hypothesize that other sources of tropical variability like convectively coupled equatorial waves (e.g., Kiladis et al. 2009) are also potential drivers of CENS. Some equatorially trapped waves, such as Mixed-Rossby Gravity (MRG) and equatorial Rossby (ER) waves, induce circulation anomalies along the equator that may promote CENS occurrences. A theoretical view of MRG wave exhibits a clear cross-equatorial flow between its dipole pressure centers (Matsuno 1966; Yanai and Maruyama 1966). On the other hand, despite that an ideal ER wave structure shows no cross-equatorial flow, observed ER wave activity in boreal winter depicts northerly component of low-level wind in the equatorial western Maritime Continent (Ferrett et al. 2020; Lubis and Respati 2021), possibly owing to the asymmetry in deformed low pressure centers.

With regard to the impact of CENS, Maulana et al. (2023) recently revealed more detailed CENS-induced precipitation anomalies that show a contrasting pattern between coastal areas and inland of Java Island. Under CENS event, the northern coastal areas (Jakarta and its vicinity) experience wet anomalies, consistent with many past studies (e.g., Trilaksono et al. 2012; Yulihastin et al. 2020, 2022). In contrast, the mountainous regions in the inland show dry anomalies (Maulana et al. 2023). As CENS with different forcings may cause different precipitation responses, investigating the variability of precipitation anomalies is necessary to understand the degree of CENS impact in the Maritime Continent.

In the current study, we aim to investigate the climatology of CENS events by identifying various potential drivers beyond the extratropical cold surge, particularly those related to tropical variability. Section 2 shows data and method used in this study. Section 3 summarizes basic characteristics of CENS events associated with CS (CENS-CS) and not associated with CS (CENS-noCS). Section 4 reveals temporal evolution of synoptic conditions related to the two groups of CENS. Section 5 presents the potential drivers of CENS-noCS. Section 6 quantifies dynamical mechanisms that trigger CENS events. Section 7 discusses the impact of CENS and flood events. Finally, section 8 highlights the important findings of this study and notes potential future studies.

2. Data and method

a. Data

We utilize the ERA5 reanalysis with 0.25° horizontal resolution (Hersbach et al. 2020) to depict circulation patterns associated with CENS. To analyze precipitation changes, we use daily precipitation data of the MSWEP V2 (Beck et al. 2019). The data, which has 0.1° horizontal resolution, is constructed by optimally merging gauges, satellites, and reanalyses and is available from 1979. Based on an intercomparison of seven precipitation datasets in Indonesia, MSWEP appears to be superior compared to others (Wati et al. 2022). To describe large-scale convection, we use daily NOAA Interpolated Outgoing Longwave Radiation (OLR) data with a horizontal resolution of 2.5° (Liebmann and Smith 1996). We also use the Real-time Multivariate MJO (RMM) index (Wheeler and Hendon 2004) and a tropical cyclone dataset from the Bureau of Meteorology of Australia. To explore the possible linkage to hydrometeorological disaster, we retrieve flood event records in Jakarta over 2002-2020 from the National Disaster Management Authority (BNPB) and rainfall data from five rain gauges in Jakarta and vicinity operated by Meteorological, Climatological, and Geophysical Agency (BMKG).

Seasonality of CS and CENS revealed by Xavier et al. (2020) shows very few occurrences in early and late winter (November and March). Therefore, this study focuses on peak winter months (December to February). The analysis period covers 41 winters from December 1979 to February 2020. To emphasize synoptic influences and to minimize data noises, a 3-day running mean smoothing is applied to all time-series data.

b. Definition of CENS events and their classification

In boreal winter, the climatological mean of monsoonal flow exhibits northerly cross-equatorial winds over the equatorial Maritime Continent that favor more precipitation in southern Indonesia and north of Australia owing to dynamical combination of the East Asian winter monsoon and the Australian summer monsoon (Ramage 1971; Chang et al. 2005b). Sub-seasonal variations of the monsoon flow are partly reflected as CENS events, which describe intermittent strengthening of northerlies in the western Maritime Continent.

CENS was often treated qualitatively as a synoptic downstream signature of subtropical or midlatitude CS (Suppiah and Wu 1998; Compo et al. 1999; Chang et al. 2005a; Aldrian and Utama 2010) until a CENS index was introduced by Hattori et al. (2011) following a robust influence of persistent CENS events on the 2007 Great Jakarta flood (Wu et al. 2007). Hattori et al. (2011) calculated a CENS index by averaging northerly sea surface winds over a wide area spanning from east of central Sumatra to eastern Java Sea. Maulana et al. (2023) then slightly modified the CENS index by narrowing the area for averaging, which focuses on the western side of Hattori et al.'s index area. The newer definition is arguably more representative to describe the impact of CENS, which is predominant over the western Java. The new index is also more convenient because removing grid points over the land area is now unnecessary since the new domain largely covers sea surface.

This study utilizes the definition of CENS index introduced by Maulana et al. (2023). It is defined as an area average of 10-m meridional wind over domain D0 (5°S-EQ, 105°-110°E; Fig. 1). A CENS event is identified when a local minimum of daily CENS index over domain D0 is below a threshold of -4.159 m s^{-1}, which is calculated from climatological average minus one standard deviation. The duration of CENS event reflects a sequence of CENS index exceeding the threshold for one day or several consecutive days. If two or more minima appear during the consecutive days, they are still considered as a single continuous event where the lowest local minimum is regarded as the peak of CENS event. A definition relative to mean climatology allows future CENS studies on intercomparison of climate models. We identify 117 CENS events over the study period according to the definition.

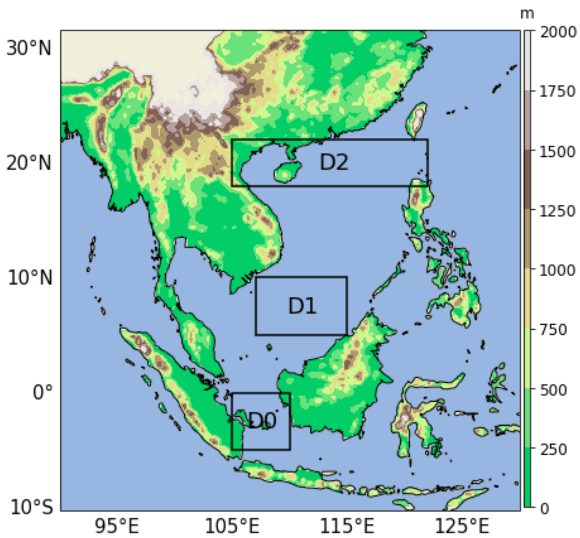

Figure 1. Location of domains for calculating CENS index (D0), SCS CS index (D1), and MSLP index (D2). Shadings indicate topography with a 250 m contour interval.

To distinguish CENS events that are and are not associated with CS, we define a set of CS criteria using the South China Sea (SCS) surge modified from Lim et al. (2017). A CENS event preceded by CS (i.e., CENS-CS event) is classified when the following criteria are satisfied: 1) 925-hPa wind over domain D1 (5°-10°N, 107°-115°E) is northeasterly and it exceeds the 0.5 standard deviations above the climatological mean (11.79 m s^{-1}) occurring on the same day or the previous day of local maximum of CENS index (day 0 or day -1); and 2) mean sea level pressure (MSLP) in the northern SCS (domain D2 at 18°-22°N, 105°-122°E) exceeds the 0.25 standard deviations above the climatological mean (1018.03 hPa) occurring on the same day or the previous day of local maximum of CENS index (day 0 or day -1). The lagged criteria are needed due to the nature of CS that takes time to propagate from East Asia to the equatorial region (e.g., Compo et al. 1999; Abdillah et al. 2021). CENS events that do not satisfy either one or both of criteria are classified into CENS-noCS events. Note that, we employ the approach of surge events instead of surge days as shown in some studies (Chang et al. 2005a; Lim et al. 2017; Maulana et al. 2023) to allow us analysing temporal atmospheric evolution, which provides indications of leading and impact pattern. Out of the 117 CENS events, we identify 69 CENS-CS and 48 CENS-noCS events. Tables S1 and S2 of the Supplemental Material show details of CENS events.

c. Identification of synoptic phenomena associated with CENS-noCS

Since CENS occurs in the tropics and CENS-CS represents events that are induced by extratropical forcing, CENS-noCS is likely to be controlled by tropical variabilities. In this study, we consider several tropical synoptic phenomena that have been shown to exert significant changes in circulation over the Maritime Continent: the Madden-Julian Oscillation (MJO) and two equatorial waves, which are equatorial Rossby (ER) and Mixed-Rossby Gravity (MRG) waves. Another prominent equatorial wave such as Kelvin wave is currently not considered because its anomalous circulation appears to hinder CENS development (Supplemental Material Fig. S1). Furthermore, we also consider tropical cyclones (TC) in the south of Indonesia because the existence of a low-pressure center over there serves as an important dynamic factor of CENS, as will be shown later.

MJO, ER wave, and MRG wave have unique zonal propagation features and therefore objective identifications of their propagation phases need to be defined. For the MJO, we utilize the eight MJO phases from the RMM index (Wheeler and Hendon 2004). Only days with MJO amplitude greater than 0.5 are considered as MJO days. To detect MRG and ER waves, we perform the wave-filtering method of Wheeler and Kiladis (1999) on tropical OLR anomalies. Based on the filtered OLR, local MRG and ER indices are constructed to quantitatively examine the relationship between the waves and CENS occurrences. The areas for indices calculation are determined based on high correlation maps between the filtered OLR field and CENS index. The local phases and amplitudes of equatorial waves are then retrieved based on wave-phase diagrams proposed by Riley et al. (2011). MRG and ER waves are considered active when their amplitudes exceed their climatological mean. To detect TC events, we collect any TC occurring in the southeastern Indian Ocean or north of Australia. A TC day is labelled when TC stage is classified as tropical disturbance or higher.

A statistical significant test is carried out to assist us in delineating areas of importance associated with CENS. We employ the significance test of Monte Carlo bootstrap method (Efron and Tibshirani 1993; Li et al. 2016).

3. Statistical comparison between CENS-CS and CENS-noCS events

Table 1 summarizes the occurrence characteristics of CENS events. Out of 117 CENS events identified over 41 boreal winters, 69 events (59%) are related to cold surges (CENS-CS) and 48 events (41%) are unrelated to cold surges (CENS-noCS). Therefore, every year CENS-CS slightly occurred more often than CENS-noCS. CENS-CS tends to last longer than CENS-noCS; and the average magnitude of CENS-CS is somewhat stronger than CENS-noCS. Overall, CENS-CS looks more active, more long-lasting, and impactful than CENS-noCS but the differences seem not large.

Parameter	CENS	CENS-CS	CENS-noCS
Number of event (events)	117	69	48
Mean frequency (events/season)	2.85	1.68	1.17
Total duration (days)	596	367	229
Mean duration (days/event)	5.09	5.32	4.77
Mean magnitude (m/s)	-5.11	-5.25	-4.9

Table 1. Statistics of CENS, CENS-CS, and CENS-noCS occurrences in terms of number of event, mean frequency, total duration, mean duration, and mean magnitude.

Probability distributions in Figs. 2a,b describe in detail the differences in duration and magnitude. The duration of CENS-noCS is more skewed to the left indicating many events lasting in a short period (1-2 days). Meanwhile CENS events lasting over 3 days or more are dominated by CENS-CS. Few CENS events can last more than 10 days up to 3 weeks. In magnitude distributions, CENS-noCS appears to dominate the magnitude weaker than -4.75 m/s. CENS-CS generally has higher probability than CENS-noCS for the magnitude stronger than -4.75 m/s, including the outliers or extreme events.

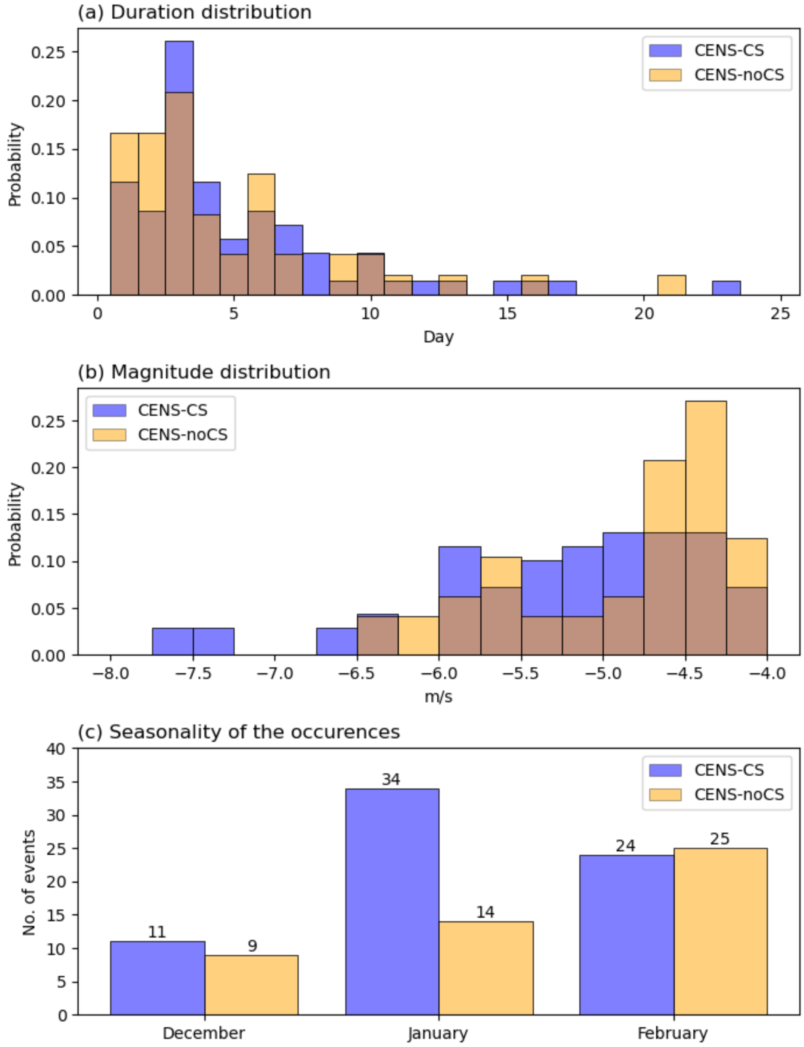

Figure 2. Probability distribution of (a) duration and (b) magnitude of CENS-CS and CENS-noCS. Panel (c) shows seasonality of the occurrences.

Seasonality of CENS occurrences is shown in Fig. 2c. CENS in December are less frequent, likely due to weaker background northerly wind and less cool of sea surface temperature in the southern South China Sea compared to January and February (Hattori et al. 2011; Koseki et al. 2013). Most CENS-CS events are observed in January, consistent with the peak period of cold surge days in the South China Sea (Lim et al. 2017). January is also the peak period of East Asian winter monsoon and Siberian High (Chan and Li 2004). Meanwhile, CENS-noCS events are mostly identified in February.

4. Temporal evolution of associated atmospheric conditions

a. CENS-CS event

Figure 3a shows low-level circulation anomalies from day -4 to day +4 of CENS-CS events with day 0 denoting the day of maximum CENS index. The evolution of MSLP and

925-hPa wind anomalies exhibits a typical propagation of East Asian cold surge that emerges from north of Tibetan Plateau (day -4) and then extends toward Southeast Asia and the North Pacific (day +2), except that the southward propagation is much clearer and connected into the Southern Hemisphere compared to previous studies that investigated CS in general (e.g., Zhang et al. 1997; Abdillah et al. 2021). Based on hovmöller diagrams in Fig. 4a, anomalous high pressure, northerly wind, and cold air clearly show southward propagation to the tropics. Approximately north of 20°N, the propagation speed of northerly wind anomalies appears to be equivalent to the propagation speed of high pressure and cold anomalies. This signature is suggested by Compo et al. (1999) as a shelf-wave mechanism. However south of 20°N, the southward propagation of northerlies appears to be much faster than pressure and temperature anomalies. This pattern is suggested as a gravity-wave response while the surge entering the South China Sea (Chang et al. 1983; Compo et al. 1999).

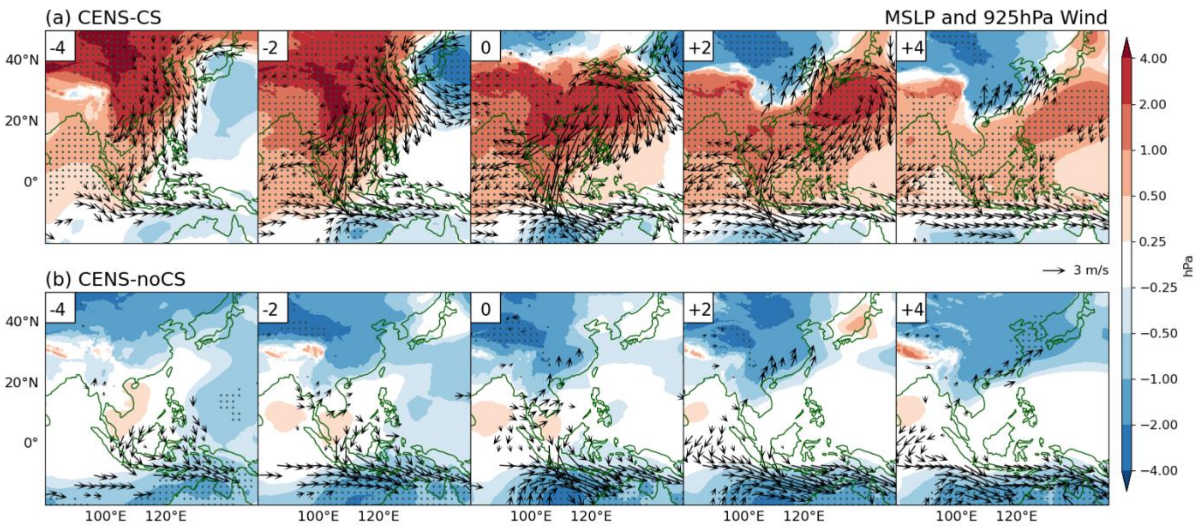

Figure 3. Temporal evolution of anomalies of 925-hPa wind (vector) and MSLP (shaded) associated with (a) CENS-CS and (b) CENS-noCS from day -4 to day 4. Day 0 indicates the maximum magnitude of CENS index. Dotted areas and vectors denote 99% confidence level of MSLP and wind field anomalies, respectively.

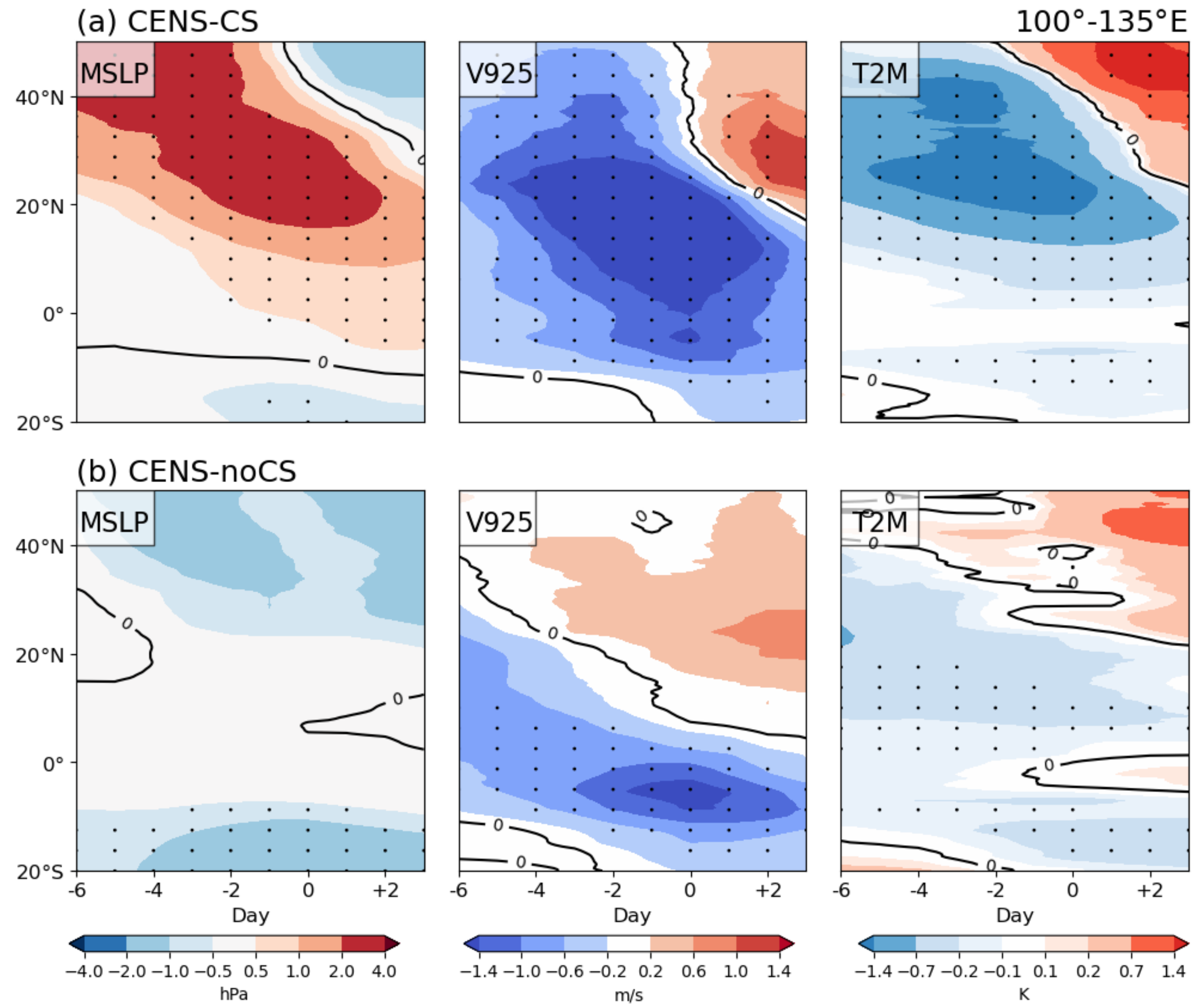

Figure 4. Hovmöller diagrams (day vs latitude) of anomalous MSLP, 925-hPa meridional wind, and 2-m temperature associated with (a) CENS-CS and (b) CENS-noCS. The anomalies are calculated from longitudinal average over 100°-135°E. Day 0 indicates the peak of CENS index. Dotted areas denote 99% confidence level.

Cold surges in the South China Sea usually induce a V-shaped precipitation response elongating from Peninsular Malaysia to Borneo (Lim et al. 2017). However, for cold surges that develop into CENS, the precipitation anomalies show a distinct west-east dipole pattern where the Peninsular Malaysia and Sumatra are drier and northern Borneo is wetter (Fig 5a). This dipole pattern was unclear in Hattori et al. (2011) but robust in Xavier et al. (2020). Meanwhile the increase in precipitation over north of Java is evident and the largest at day 0, consistent with previous studies (e.g., Hattori et al. 2011).

The increase and decrease in precipitation are closely correlated with anomalous moisture flux convergence and divergence, respectively (Fig. 6a). Northern Borneo exhibits convergence anomalies due to the confluence of northerlies and northeasterlies over the north of Borneo mountains. In contrast, in Peninsular Malaysia, the climatological northeasterlies are weakened and deflected toward the south of equator, resulting in a reduction in incoming moisture fluxes and an increase in anomalous divergence. In northern Java, the convergence is mostly induced by the interaction of enhanced northerlies and topography.

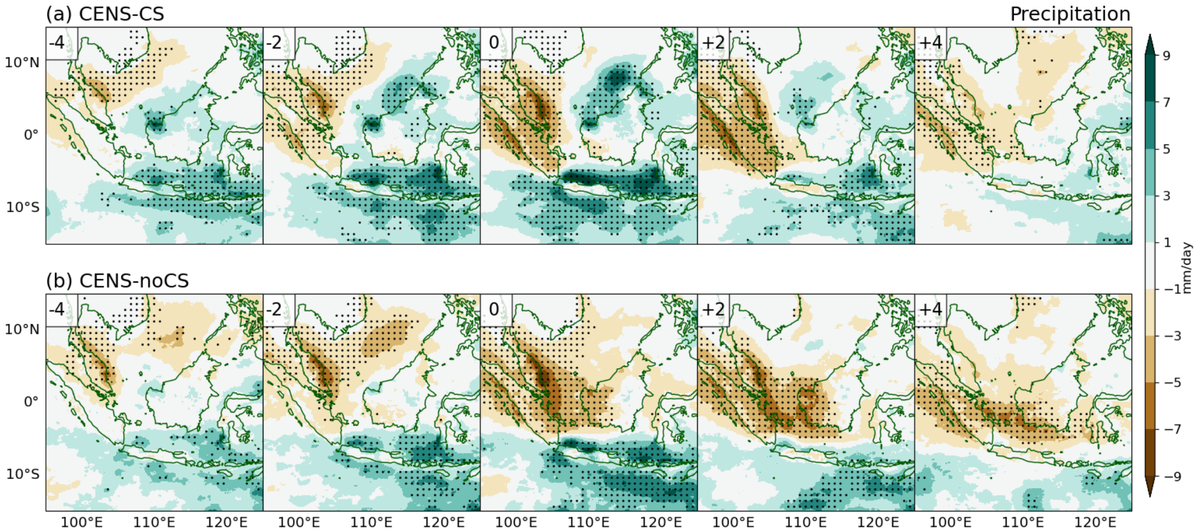

Figure 5. Temporal evolution of anomalies of precipitation (shaded) associated with (a) CENS-CS and (b) CENS-noCS from Day -4 to Day 4. Day 0 indicates the maximum magnitude of CENS index. Dotted areas denote 99% confidence level based on a two-sided Student's t test.

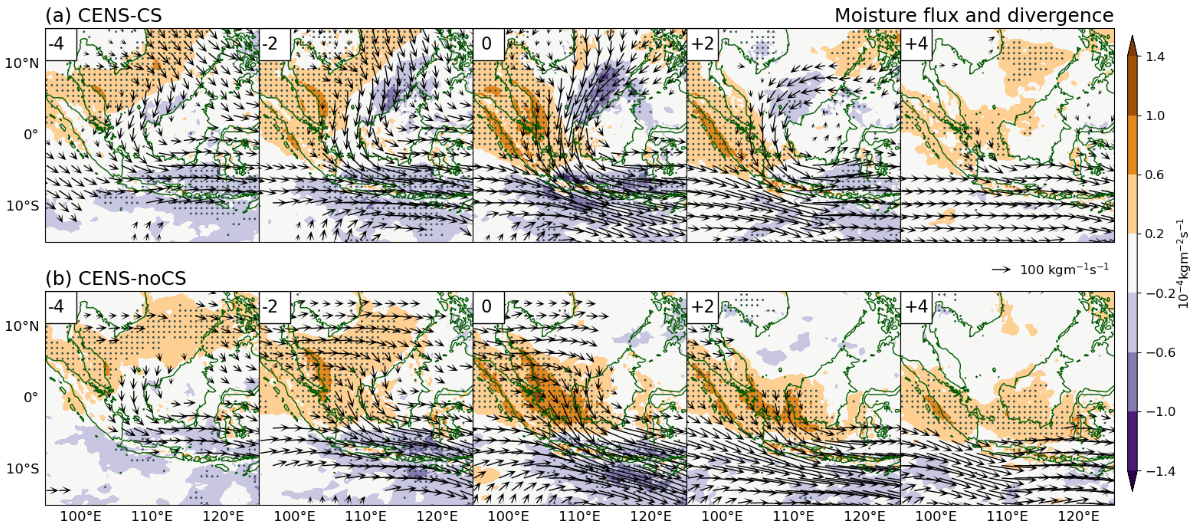

Figure 6. Temporal evolution of anomalies of moisture fluxes (vector) and its divergence (shading) associated with (a) CENS-CS and (b) CENS-noCS from Day -4 to Day 4. Day 0 indicates the maximum magnitude of CENS index. Dotted areas and vectors denote 99% confidence level of divergence and moisture flux anomalies, respectively, based on a two-sided Student's t test.

b. CENS-noCS event

During CENS-noCS events, no high-pressure anomalies are observed in the north or east of Tibetan Plateau. Instead, significant low-pressure anomalies appear over there (Fig. 3b). A small anomalous high-pressure center exists in the South China Sea, but the signal is statistically insignificant. An interesting feature of CENS-noCS is large low-pressure anomalies south of Indonesia, which reach a peak at day 0, indicating an important condition of CENS events. The low-pressure signature is also present in CENS-CS but with a weaker magnitude (Fig. 3a).

Figure 5b shows precipitation anomalies associated with CENS-noCS events. Northern Java exhibits a significant increase in precipitation, especially at day 0 in the northwestern part. This pattern is similar to the response in CENS-CS although the magnitude seems a little bit weaker, and the coverage looks smaller. Interestingly in the north of 5°S, the anomalous precipitation pattern is quite different from that in CENS-CS. The regions of Sumatra, Peninsular Malaysia, and Borneo show consistent decrease in precipitation (Fig. 5b, day 0). Unlike CENS-CS, the anomalous moisture flux pattern over north of Borneo shows no northeasterlies (Fig. 6b), which are necessary for the formation of forced convection over northwestern Borneo. The northerly anomalies of CENS emerge from approximately 2.5°N, spanning from Sumatra to west of Borneo. Subsequently, their magnitude increases farther south, indicating that the anomalous divergence of CENS-noCS in Sumatra-Borneo is a result of a southward acceleration of the anomalous northerlies.

5. Potential drivers of CENS-noCS

a. MJO

This section investigates the possibility of MJO inducing CENS. Figure 7a exhibits composite anomalies of OLR and low level circulations associated with four MJO phases from combination of the eight MJO phases of Wheeler and Hendon (2004). The composite maps give us some hints on which phases the atmospheric conditions are favorable for CENS development. Over the seas between Sumatra and Borneo, the composite anomalies show increase in northerlies in phases 4-5 and 6-7 but anomalous southerlies appear in phases 1,8 and 2-3. This variation in background condition is consistent with distribution of CENS-noCS events within MJO phases (Fig. 7b,c), especially phases 6-7 when the strengthened northerlies are clearer (Fig. 7a). Phases 4-7 account for a large 40 CENS-noCS events. This finding is different with previous studies that directly made a connection of CENS to particular MJO phases 3 and 4 over the western Maritime Continent (Hattori et al. 2011; Xavier et al. 2020).

MSLP anomalies of the MJO in Fig. 7a suggest that meridional gradient of pressure anomalies between the southern SCS and south of Indonesia dynamically drives the northerlies over CENS region. In phases 4-5, the meridional gradient is largely supported by low-pressure anomalies center south of Indonesia. Meanwhile in phases 6-7, the gradient is controlled by seesaw of high-pressure anomalies in the South China Sea and moderate low-pressure anomalies in south of Indonesia, facilitating greater southward pressure gradient force. The feature of equatorial north-south pressure gradient and its northerlies is distinct from the geostrophic feature of cold surge in the midlatitudes (e.g., Shoji et al. 2014).

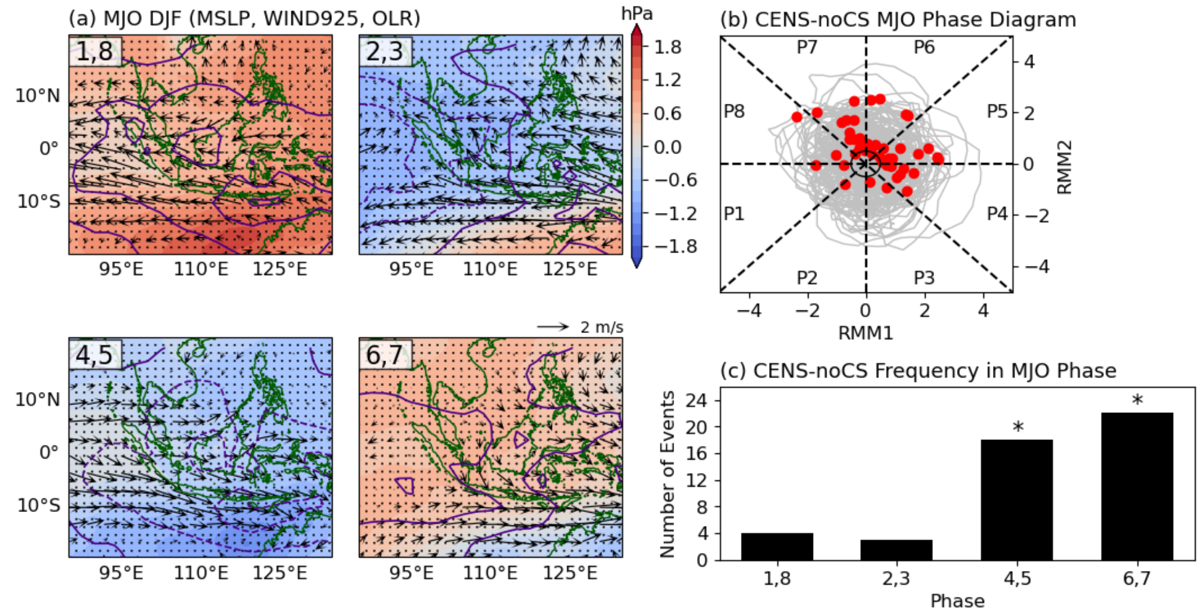

Figure 7. (a) Composite of MSLP (shading), 925-hPa wind (vector), and OLR anomalies (purple contour) during the eight phases of MJO. Dotted areas and vectors denote 99% confidence level of MSLP and wind field anomalies. (b) Historical MJO activity (grey lines) and CENS-noCS incidents at day 0 (red circles) in the MJO RMM phase-space diagram over the study period. Black circle in the center denotes MJO magnitude of 0.5. (c) Distribution of CENS-noCS occurrences arranged based on the phases of MJO whose magnitudes greater than 0.5. The asterisks indicate the number of events exceeding confidence level of 99%.

Previous studies usually emphasize the impacts of MJO on Indonesia during phases 4 -5 for large-scale convection (Wheeler and Hendon 2004); and during phases 2-3 or 3-4 for heavy precipitation over land (Peatman et al. 2014; Muhammad et al. 2021). In phases 6-7, typically, the great cluster of deep convections already shifts eastward to the western Pacific, transitioning into “dry phase” over the Maritime Continent. Therefore, the evidence on the increased CENS activity during MJO phases 6 and 7 raises a challenging question whether those CENS-noCS events cause impact on precipitation or not.

The MJO impact on Indonesian rainfall is quite inhomogeneous, especially over land. Circulation anomalies induced by MJO can interact with local circulation and topography, resulting a more complex precipitation response (Hsu and Lee 2005; Hidayat and Kizu 2010; Kim et al. 2017). Qian (2020) examined the MJO impact over Java Island in detail. He found that the MJO precipitation increases in phases 2-3 only appear over inland or mountains, while the increase over northern coast of Java appear in phases 6-7 (Fig. 5 in Qian 2020), consistent with the peak frequency of CENS-noCS in (Fig. 7c). Other studies by Peatman et al. (2014) and Lim et al. (2017) also showed positive precipitation anomalies in northern coast of Java during the both phases. This pattern is also confirmed by ground observation analysis conducted by a previous study, which documented that daily mean and extreme precipitation over Jakarta is amplified in the austral summer MJO phases 6-8 after falling in phases 3-5 (Lestari et al. 2019). In fact, the great Jakarta flood in 2013 was coincided with the MJO phase 6 that was transitioning into phase 7 and was accompanied by incoming northwesterlies from Java Sea (Wu et al. 2013).

b. Equatorial waves

To investigate the relationship between CENS and MRG wave activity, we define a local MRG index from difference of filtered OLR anomalies in the north and south of equator (Fig. 8a). Figure 8b shows composites of OLR and low-level circulation anomalies associated with four local phases of MRG, which are defined according to the combination of the OLR index and its tendency. Clear northerly anomalies are shown in MRG phase 1 when positive OLR anomalies reside over the SCS and negative OLR anomalies present over Java and, which are accompanied by a seesaw of pressure anomalies off the equator. This pattern is consistent the theoretical structure of MRG (e.g., Kiladis et al. 2009). In other phases, the anomalous northerly over CENS area is not apparent. Figures 8c and 8d confirm that MRG phase 1 significantly exhibit most of CENS-noCS occurrences. We identify 11 CENS-noCS events coincided with MRG phases 1.

Next, we investigate the possibility of ER wave in affecting CENS-noCS events. A local ER index and its four phases are defined in similar way with the MRG wave (Fig. 9a). From the composite maps of filtered anomaly fields (Fig. 9b), the symmetric features of OLR or pressure anomalies are evident, but their magnitudes and area coverages are different between the Northern and Southern Hemispheres. These asymmetric conditions promote cross-equatorial flows, which were also depicted in the results of Ferrett et al. (2020) and Lubis and Respati (2021). Figure 9b suggests that ER phase 1 provides the most favorable background conditions for CENS. These associations are consistently shown by a distribution of CENS-noCS events over the four phases of ER (Fig. 10c,d). We find 17 CENS-noCS events co-occurring with the ER phases 1.

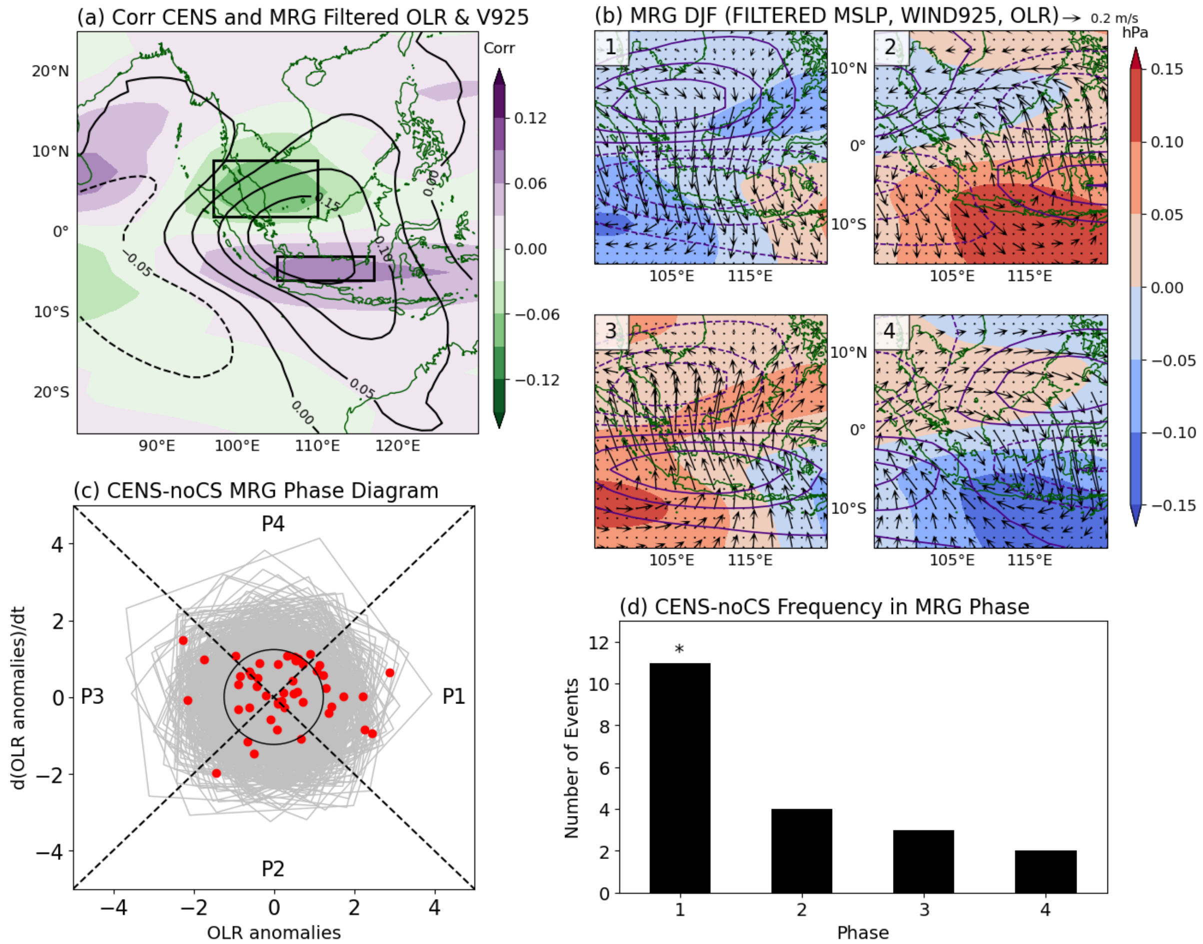

Figure 8. (a) Simultaneous correlation coefficients between daily CENS index and MRG-filtered OLR (shading) and 925-hPa meridional wind (contour). Two black rectangles denote areas for calculating an MRG index to determine local wave patterns. (b) Composite of filtered MSLP (shading), 925-hPa wind (vector), and OLR anomalies (purple contour) anomalies during the four phases of MRG wave in the western Maritime Continent. Dotted areas and vectors denote 99% confidence level of MSLP and wind field anomalies, respectively. (c) Historical MRG activity (grey lines) and CENS-noCS incidents at day 0 (red circles) in the phase-space diagram over the study period. Black circle in the center denotes the climatological mean of the index. (d) Distribution of CENS-noCS occurrences arranged based on the phases of MRG. The asterisks indicate the number of events exceeding confidence level of 99%.

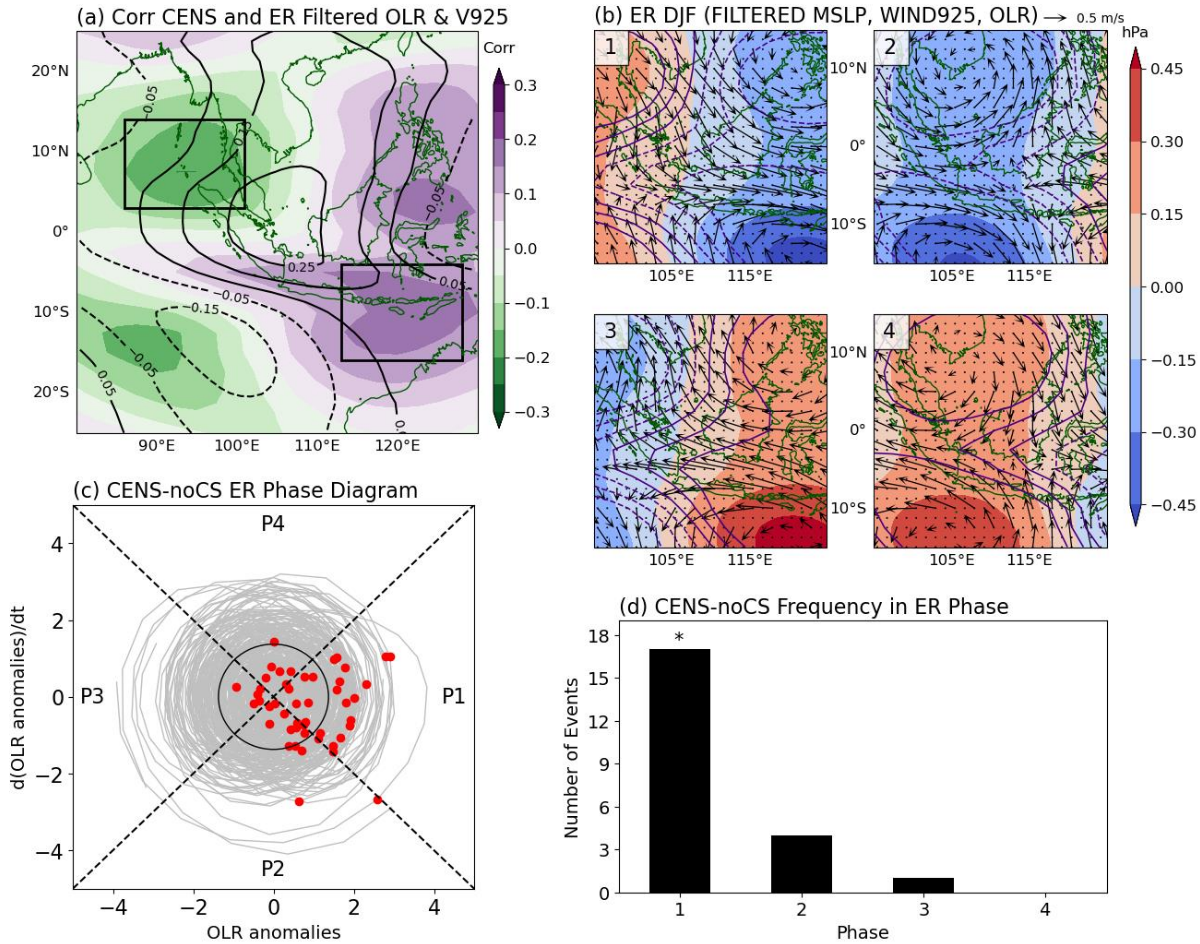

Figure 9. As in Fig. 8, but for ER wave.

c. Tropical cyclones

Anomalous MSLP field of CENS-noCS shows low-pressure anomalies over south of Indonesia (Fig. 3b), suggesting that a low-pressure system such as tropical cyclone (TC) may also have an impact on the development of CENS. A case study by Saufina et al. (2021) noted a CENS event occurred in last February 2020 was coincided with a TC in the southeastern Indian Ocean. They suggested that the TC played a role in inducing the southward flow toward the south of Java.

We find that 18 CENS-noCS events were associated with TCs over south of Indonesia. A list of identified TC names and dates is shown in Table S3. The locations of TC center at day 0 of CENS are shown in Fig. 10a. Since the locations of TCs are quite diverse spatially, the resulting composite analysis may undermine some circulation anomalies of the TCs. To avoid such condition, we perform K-means clustering method to localize the TCs. By using Elbow method, we determine two TC clusters that represent western and eastern TCs across south of Indonesia.

The two TC clusters consistently show northerly anomalies over the CENS region, even though the locations of the low-pressure center differ between the clusters (Fig. 12b). As noted previously, the main synoptic pattern of CENS is the meridional pressure gradient between the southern SCS and the south of Indonesia. The deepened low-pressure center of TC provides this gradient and facilitates northerly anomalies from the equator.

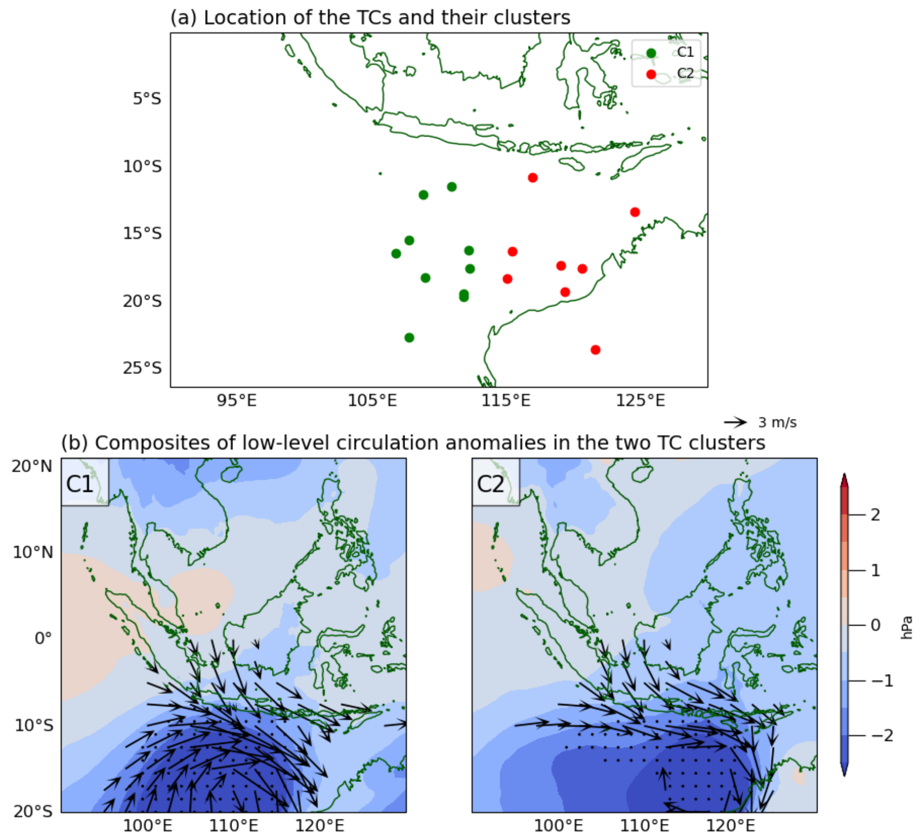

Figure 10. (a) Location of TC that are associated with CENS-noCS events. Different colors indicate different clusters of TC constructed from K-means clustering. (b) Composites of MSLP (shading) and 925-hPa wind (vector) according to the two clusters. Dotted areas and vectors denote 99% confidence level of MSLP and wind field anomalies, respectively.

6. The significance of meridional pressure gradient force

The previous figures show evidence of meridional pressure gradient force in controlling CENS events. To confirm its significance, we quantify the pressure gradient and its relationship with CENS. Figure 11a shows a strong correlation between the meridional pressure gradient index and CENS index at day 0 (r=-0.67). The pressure gradient index is defined from regression coefficients of zonally-averaged MSLP anomalies over 105°-110°E along 10°S to 5°N. Both CENS-CS and CENS-noCS show similar relationships: the greater the pressure difference, the stronger the northerlies.

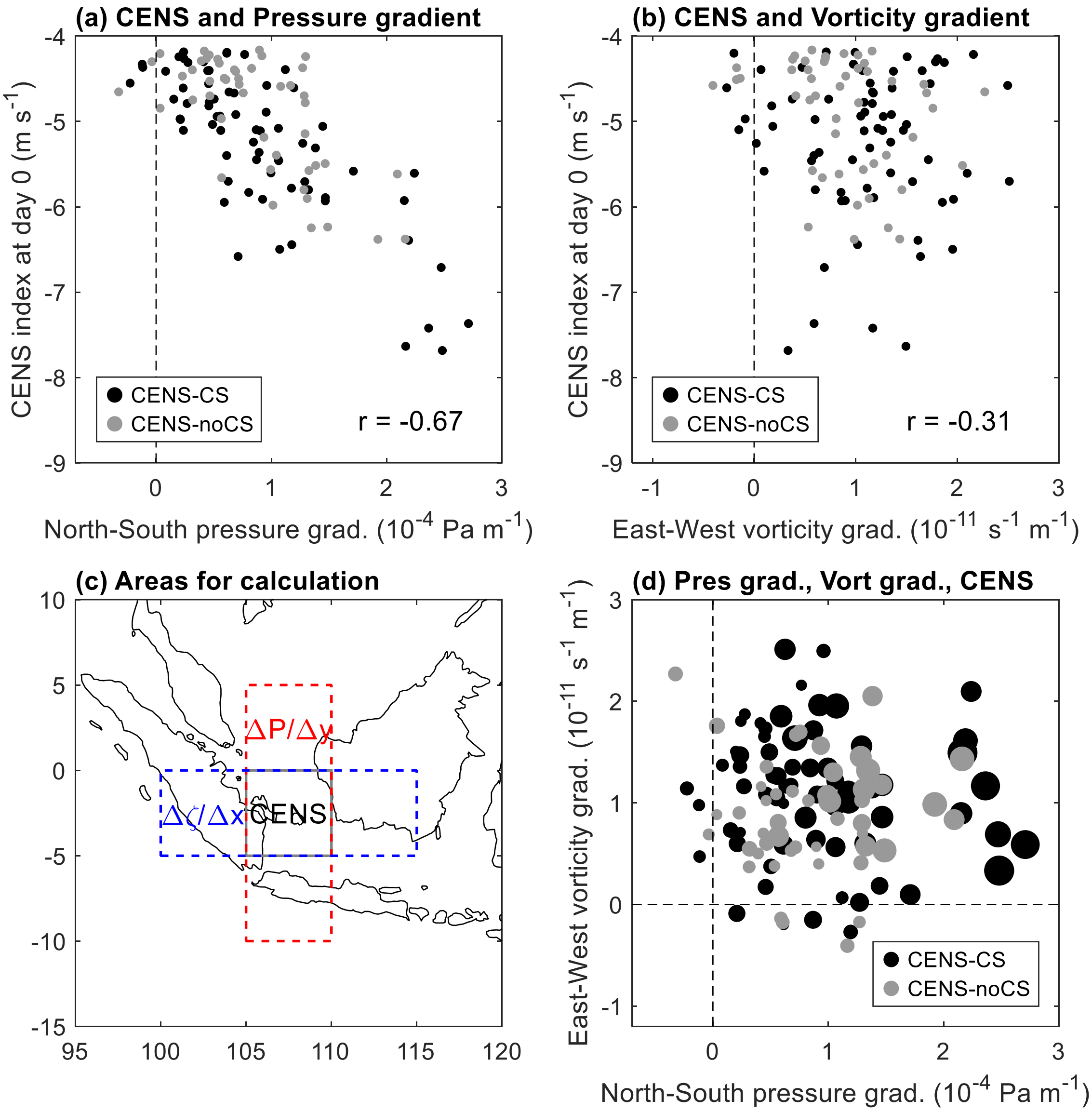

Figure 11. (a) Relationship between meridional pressure gradient index (red box in c) and CENS index at day 0 of CENS events. The correlation coefficient *r* is shown inside the panel. (b) As in a but with zonal vorticity gradient index (blue box in c). (c) Bounding boxes for the gradients and CENS index. (d) Distribution of CENS index as a function of pressure and vorticity gradients. The size of circles indicates the strength of CENS.

The meridional gradient is in contrast with the well-developed view of extratropical cold surge dynamic, which is mainly controlled by zonal gradient of high pressure in Siberia and low pressure in the North Pacific (e.g., Compo et al. 1999; Shoji et al. 2014). This difference is expected since CENS occurs in low Coriolis force region, although the geostrophic effect is still apparent as indicated by the northern flank of low-pressure center in south of Indonesia that facilitates westerly component of CENS over the Java Sea (Figs. 3 and 5).

The north-south pressure gradient should have positive values to promote CENS but a few CENS events show a negative pressure gradient (Fig. 11a). Theoretically, meridional wind near the equator can also be induced by tropical vortices, which are usually evident in equatorial waves patterns. By considering the CENS region located just south of equator, the favorable condition for the northerlies is negative vorticity in the west and positive vorticity in the east. To investigate whether the CENS events associated with the negative meridional pressure gradient are linked to the vortex-induced circulation, we calculate zonal vorticity gradient index defined by regression coefficients of meridionally-averaged vorticity anomalies over Sumatra to Borneo Islands (100°-115°E, 5°S-EQ; Fig. 11c). Figure 11d suggests that is possibly the case because all CENS events occurred either under a positive north-south pressure gradient or/and a positive east-west vorticity gradient. The combination of these two dynamical factors seems to contribute positively to the strength of CENS. However, the zonal vorticity gradient is regarded as the secondary factor because its overall correlation with the CENS index is relatively weaker compared to the meridional pressure gradient (Fig. 11a,b).

7. CENS linkage to flood events

This section discusses relationships between CENS, Jakarta rainfall, and Jakarta flood (Fig. 12). A flood event is related to CENS if it occurred between two days before and two days after CENS day. Out of 56 CENS events over DJF 2001/02 to 2019/20 (period of available flood reports), 24 were associated with flood events. 18 (6) of them occurred on the same day or after (prior to) the peak of CENS, respectively. The reason for floods occurring before the peak of CENS is possibly due to a slow onset in some CENS events. Table S4 in the Supplemental Material lists the details of flood events.

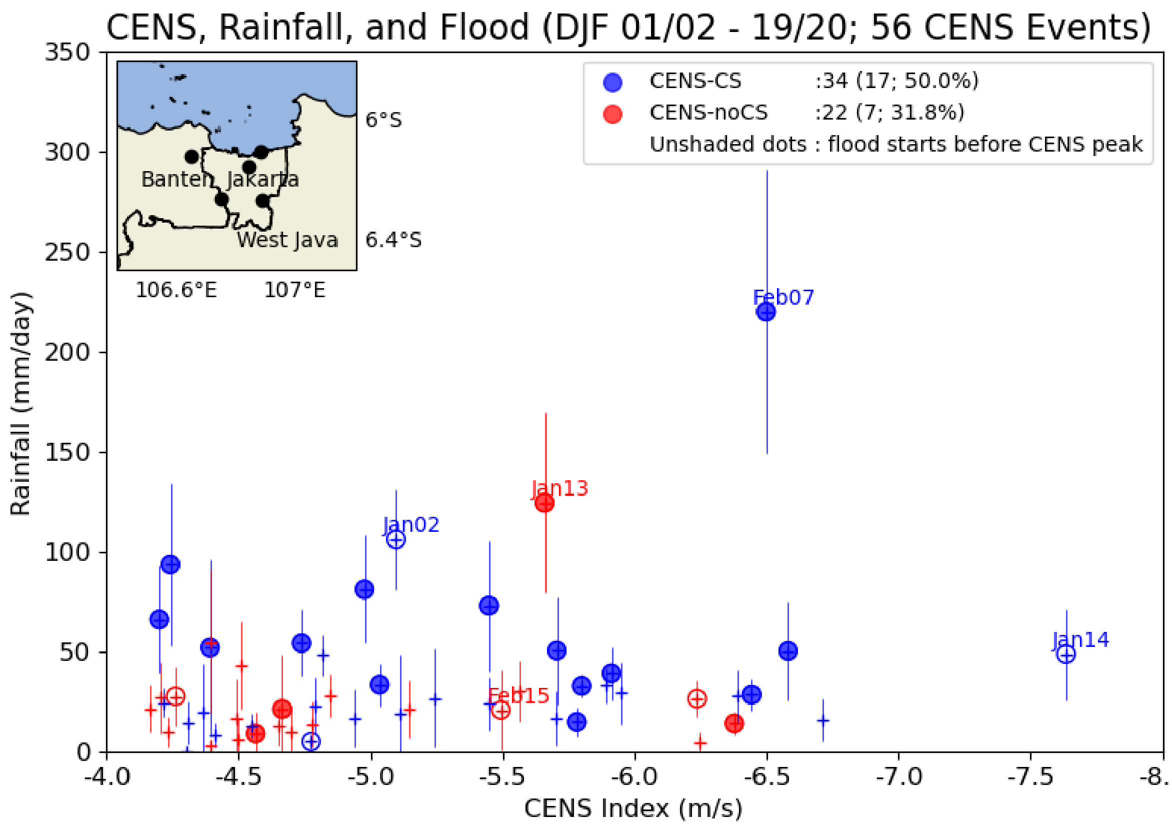

Figure 12. Relationship between the magnitude of CENS events and Jakarta rainfall from DJF 2001/02 to DJF 2019/20 (the period of available flood records). Circles indicate the events when floods were reported. Shaded and empty circles denote floods that started after and prior to the peak of CENS, respectively. Blue and red colors denote CENS-CS and CENS-noCS events, respectively. The rainfall data are based on five ground stations whose locations are shown in the map on the top-left side of the image. Vertical lines denote rainfall variation among the stations denoted by mean ± standard deviation. Text labels near the circles indicate the month and the year of several major floods.

The relationship graph shows that CENS-CS tends to cause larger rainfall in Jakarta than CENS-noCS (Fig. 12). The areal averages of observed rainfall during CENS-CS and CENS-noCS range from approximately 5-220 mm day^{-1} and 8-120 mm day^{-1}, respectively. We note that several flood events seem to be associated with low rainfall amounts. There are two possible reasons. One is due to the limited number of stations, which may not well capture localized high-intensity rains. Another is due to the rainfall occurring in the upstream areas in south of Jakarta. Nevertheless, flood events, including the major ones, can occur during either CENS-CS or CENS-noCS events, highlighting the importance of both CENS types in hydrometeorological disasters in the capital.

8. Concluding remarks

This study evaluates the climatology of CENS events according to their potential drivers of extratropical and tropical origins. We identify that 41% of CENS events are not linked to extratropical East Asian cold surges (CENS-noCS), confirming the results of previous studies. We further investigated those CENS-noCS events in more details and find that zonally propagating tropical variability associated with Madden-Julian Oscillation (phases 4-7), mixed-Rossby gravity waves, and equatorial Rossby waves are possible driver of CENS. Another potential driver of CENS is the tropical cyclones that are developing or developed in north of Australia.

We analyzed the mechanisms of how these tropical phenomena may induce CENS events. The results show that lower circulation anomalies exhibit a clear coincidence with north-south pressure gradient force between the South China Sea and south of Indonesia. This gradient is more obvious in CENS-noCS compared to that in CENS-CS. On averages, this feature characterizes all of the identified CENS-noCS with variation in the strength of high-pressure and low-pressure centers. Moreover, the statistical correlation between the meridional pressure gradient force and CENS index is quite strong, implying the importance of this pattern, which is distinct to the zonal pressure gradient force in the extratropics. However, a few CENS events occurred under weak, or even negative, north-south pressure gradient. For these cases, the strengthening of northerly wind is more likely driven by positive zonal vorticity gradient, while its role could be of secondary importance in the presence of moderate-to-strong pressure gradient force

We also find that CENS-noCS events have significant hydrometeorological impacts. The CENS-noCS composite precipitation show positive anomalies over the northern coast of Java Island albeit relatively weaker than those in CENS-CS. Nevertheless, flood events in Jakarta can happen during both types of CENS, suggesting the forecasters to monitor and forecast all CENS events regardless of their origin. Thus, our identification of CENS drivers beside the cold surges may be useful monitoring and predicting weather and climate over the Maritime Continent, especially CENS-related high impact weather events.

Topics regarding CENS are quite broad, and this study only covers certain aspects of CENS. The tropical variabilities can interact with each other and thus result in more complex signatures. For example, Lubis and Respati (2021) showed that the impact of MJO is sensitive to the presence of equatorial waves and vice versa. Such topics are beyond the scope of the current study. The current study also did not consider the possibility of interactions between CENS-CS and tropical phenomena. A number of studies documented that MJO over the western Maritime Continent enhance CENS-CS and amplify its impact over northern Java (Hattori et al. 2011; Xavier et al. 2020; Trismidianto et al. 2023; Satiadi et al. 2023). A recent study by Diong et al. (2023) showed the importance of ER waves on changes in cold surge characteristics over the South China Sea and potentially its cross-equatorial flow. Other potential factors that may have impact, positively or negatively, on CENS-noCS are the South China Sea “cold tongue” (Koseki et al. 2013; Yulihastin et al. 2020; Seow et al. 2023), Borneo Vortex (Chang et al. 2005a; Koseki et al. 2014), and the recently discussed Quasi-Biweekly Oscillation (Dong et al. 2022), which are worth to be explored in the future. A comprehensive future study is needed to carefully review all the possible interactions between CENS and other phenomena. In addition, the mesoscale feature of precipitation and response of diurnal cycle on the presence of CENS (Mori et al. 2018; Yulihastin et al. 2022; Satiadi et al. 2023) are also important since it is crucial in determining the location and timing of torrential rainfall. Predictability of such response in numerical models is a challenging topic. In a regional model study, Yulihastin et al. (2022) was able to capture the mesoscale propagation of CENS-induced rainfall but failed in representing its coverage and precise timing. Xavier et al. (2020) noted persisting dry bias over a large part of the western Maritime Continent, which is partly attributed to its seasonal bias. Furthermore, CENS may have large-scale implications, as indicated by the classical study of CS by Chang and Lau (1980). CENS-CS can give feedback to the structure and intensity of MJO through the enhanced large-scale moisture flux convergence over the southern Maritime Continent (Lubis et al. 2023), which may subsequently affect the downstream propagation of MJO and its teleconnections. In a longer time scale, interannual climate variability, such as El Nino-Southern Oscillation (Trenberth 1997) and Indian Ocean Dipole (Saji et al. 1999), or even decadal-multidecadal forcing (Pang et al. 2023) and global warming effect may modulate and alter the activity of CENS.

Acknowledgments

We are grateful to three anonymous reviewers for their insightful comments and suggestions to improve the quality of the manuscript. This research is partly supported by Collaborative Research Program of the Faculty of Earth Science and Technology (PPMI Kolaboratif FITB-ITB) (grant number: 605/IT1.C01/SK-TA/2022) and Institute of Research and Community Services of Institut Teknologi Bandung. We would like to thank colleagues in Atmospheric Science Laboratory, Tohoku University, for giving insightful comments and suggestions during the corresponding author visit in 2023.

Data Availability Statement

The ERA5 daily data are obtained from the ERA5 online daily statistic calculator (https://cds.climate.copernicus.eu/apps/user-apps/app-c3s-daily-era5-statistics), which uses ERA5 hourly single level (https://doi.org/10.24381/cds.adbb2d47) and pressure levels (https://doi.org/10.24381/cds.bd0915c6). The daily MSWEP V2 dataset is from https://www.gloh2o.org/mswep/. The NOAA OLR data is from https://psl.noaa.gov/data/gridded/data.olrcdr.interp.html. Two datasets are obtained from Bureau of Meteorology, Australia: MJO data (http://www.bom.gov.au/climate/mjo/) and TC data (http://www.bom.gov.au/cyclone/tropical-cyclone-knowledge-centre/databases/). The rain gauges data are obtained from https://dataonline.bmkg.go.id/home. Indonesian flood data is obtained from https://dibi.bnpb.go.id/.

REFERENCES

Abdillah, M. R., Y. Kanno, and T. Iwasaki, 2017: Tropical–Extratropical Interactions Associated with East Asian Cold Air Outbreaks. Part I: Interannual Variability. *J. Climate*, **30**, 2989–3007, https://doi.org/10.1175/JCLI-D-16-0152.1.

——, ——, and ——, 2018: Tropical–Extratropical Interactions Associated with East Asian Cold Air Outbreaks. Part II: Intraseasonal Variation. *J. Climate*, **31**, 473–490, https://doi.org/10.1175/JCLI-D-17-0147.1.

——, ——, ——, and J. Matsumoto, 2021: Cold Surge Pathways in East Asia and Their Tropical Impacts. *Journal of Climate*, **34**, 157–170, https://doi.org/10.1175/JCLI-D-20-0552.1.

Aldrian, E., and G. S. A. Utama, 2010: Identifikasi Dan Karakteristik Seruak Dingin (Cold Surge) Tahun 1995-2003 (in Indonesian). *Jurnal Sains Dirgantara*, **4**.

Beck, H. E., E. F. Wood, M. Pan, C. K. Fisher, D. G. Miralles, A. I. J. M. van Dijk, T. R. McVicar, and R. F. Adler, 2019: MSWEP V2 Global 3-Hourly 0.1° Precipitation: Methodology and Quantitative Assessment. *Bulletin of the American Meteorological Society*, **100**, 473–500, https://doi.org/10.1175/BAMS-D-17-0138.1.

BMKG, 2024: Northerly Cold Surge Monitoring. *Badan Meteorologi Klimatologi dan Geofisika*,. https://web.meteo.bmkg.go.id/en/pengamatan/indeks-surge.

Chan, J. C. L., and C. Li, 2004: The East asia winter monsoon. *East Asian Monsoon*, Vol. Volume 2 of *World Scientific Series on Asia-Pacific Weather and Climate*, WORLD SCIENTIFIC, 54–106.

Chang, C.-P., and K. M. W. Lau, 1980: Northeasterly Cold Surges and Near-Equatorial Disturbances over the Winter MONEX Area During December 1974. Part II:

Planetary-Scale Aspects. *Monthly Weather Review*, **108**, 298–312, https://doi.org/10.1175/1520-0493(1980)108<0298:NCSANE>2.0.CO;2.

——, J. E. Millard, and G. T. J. Chen, 1983: Gravitational Character of Cold Surges during Winter MONEX. *Monthly Weather Review*, **111**, 293–307, https://doi.org/10.1175/1520-0493(1983)111<0293:GCOCSD>2.0.CO;2.

——, P. A. Harr, and H.-J. Chen, 2005a: Synoptic Disturbances over the Equatorial South China Sea and Western Maritime Continent during Boreal Winter. *Monthly Weather Review*, **133**, 489–503, https://doi.org/10.1175/MWR-2868.1.

Chang, C.-P., Z. Wang, J. McBride, and C.-H. Liu, 2005b: Annual Cycle of Southeast Asia—Maritime Continent Rainfall and the Asymmetric Monsoon Transition. *Journal of Climate*, **18**, 287–301, https://doi.org/10.1175/JCLI-3257.1.

Chen, T.-C., J.-D. Tsay, J. Matsumoto, and J. Alpert, 2015: Development and Formation Mechanism of the Southeast Asian Winter Heavy Rainfall Events around the South China Sea. Part I: Formation and Propagation of Cold Surge Vortex*. *Journal of Climate*, **28**, 1417–1443, https://doi.org/10.1175/JCLI-D-14-00170.1.

Compo, G. P., G. N. Kiladis, and P. J. Webster, 1999: The horizontal and vertical structure of east Asian winter monsoon pressure surges. *Quarterly Journal of the Royal Meteorological Society*, **125**, 29–54, https://doi.org/10.1002/qj.49712555304.

Diong, J.-Y., P. Xavier, S. J. Woolnough, and F. A. Abdullah, 2023: Equatorial Rossby waves on cold surge days and their impact on rainfall. *Quarterly Journal of the Royal Meteorological Society*, **149**, 2031–2047, https://doi.org/10.1002/qj.4493.

Dong, Z., L. Wang, R. Yang, J. Cao, and P. Hu, 2022: Impact of Quasi-Biweekly Oscillation on Southeast Asian Cold Surge Rainfall Monitored by TRMM Satellite Observation. *Remote Sensing*, **14**, 5200, https://doi.org/10.3390/rs14205200.

Efron, B., and R. J. Tibshirani, 1993: *An Introduction to the Bootstrap*. Chapman & Hall/CRC, 456 pp.

Fajary, F. R., T. W. Hadi, and S. Yoden, 2019: Contributing Factors to Spatiotemporal Variations of Outgoing Longwave Radiation (OLR) in the Tropics. *Journal of Climate*, **32**, 4621–4640, https://doi.org/10.1175/JCLI-D-18-0350.1.

Ferrett, S., G.-Y. Yang, S. J. Woolnough, J. Methven, K. Hodges, and C. E. Holloway, 2020: Linking extreme precipitation in Southeast Asia to equatorial waves. *Quarterly Journal of the Royal Meteorological Society*, **146**, 665–684, https://doi.org/10.1002/qj.3699.

Hattori, M., S. Mori, and J. Matsumoto, 2011: The Cross-Equatorial Northerly Surge over the Maritime Continent and Its Relationship to Precipitation Patterns. *JMSJ*, **89A**, 27–47, https://doi.org/10.2151/jmsj.2011-A02.

Hermawan, E., and Coauthors, 2022: Large-Scale Meteorological Drivers of the Extreme Precipitation Event and Devastating Floods of Early-February 2021 in Semarang, Central Java, Indonesia. *Atmosphere*, **13**, 1092, https://doi.org/10.3390/atmos13071092.

Hersbach, H., and Coauthors, 2020: The ERA5 global reanalysis. *Quarterly Journal of the Royal Meteorological Society*, **146**, 1999–2049, https://doi.org/10.1002/qj.3803.

Hidayat, R., and S. Kizu, 2010: Influence of the Madden-Julian Oscillation on Indonesian rainfall variability in austral summer: INFLUENCE OF THE MADDEN-JULIAN OSCILLATION ON INDONESIAN RAINFALL. *Int. J. Climatol.*, **30**, 1816–1825, https://doi.org/10.1002/joc.2005.

Hsu, H.-H., and M.-Y. Lee, 2005: Topographic Effects on the Eastward Propagation and Initiation of the Madden–Julian Oscillation. *Journal of Climate*, **18**, 795–809, https://doi.org/10.1175/JCLI-3292.1.

Kiladis, G. N., K. H. Straub, and P. T. Haertel, 2005: Zonal and Vertical Structure of the Madden–Julian Oscillation. https://doi.org/10.1175/JAS3520.1.

——, M. C. Wheeler, P. T. Haertel, K. H. Straub, and P. E. Roundy, 2009: Convectively coupled equatorial waves. *Rev. Geophys.*, **47**, RG2003, https://doi.org/10.1029/2008RG000266.

Kim, D., H. Kim, and M.-I. Lee, 2017: Why does the MJO detour the Maritime Continent during austral summer? *Geophysical Research Letters*, **44**, 2579–2587, https://doi.org/10.1002/2017GL072643.

Koseki, S., T.-Y. Koh, and C.-K. Teo, 2013: Effects of the cold tongue in the South China Sea on the monsoon, diurnal cycle and rainfall in the Maritime Continent. *Q.J.R. Meteorol. Soc.*, **139**, 1566–1582, https://doi.org/10.1002/qj.2052.

Koseki, S., T.-Y. Koh, and C.-K. Teo, 2014: Borneo vortex and mesoscale convective rainfall. *Atmos. Chem. Phys.*, **14**, 4539–4562, https://doi.org/10.5194/acp-14-4539-2014.

Lestari, S., A. King, C. Vincent, D. Karoly, and A. Protat, 2019: Seasonal dependence of rainfall extremes in and around Jakarta, Indonesia. *Weather and Climate Extremes*, **24**, 100202, https://doi.org/10.1016/j.wace.2019.100202.

Li, W., W. Guo, P. Hsu, and Y. Xue, 2016: Influence of the Madden–Julian oscillation on Tibetan Plateau snow cover at the intraseasonal time-scale. *Sci Rep*, **6**, 30456, https://doi.org/10.1038/srep30456.

Liebmann, B., and C. a. Smith, 1996: Description of a complete (interpolated) outgoing longwave radiation datasets. *Bull. Amer. Meteor. Soc.*, **77**, 1275-1277.

Lim, S. Y., C. Marzin, P. Xavier, C.-P. Chang, and B. Timbal, 2017: Impacts of Boreal Winter Monsoon Cold Surges and the Interaction with MJO on Southeast Asia Rainfall. *Journal of Climate*, **30**, 4267–4281, https://doi.org/10.1175/JCLI-D-16-0546.1.

Liu, Q., G. Chen, L. Wang, Y. Kanno, and T. Iwasaki, 2021: Southward cold airmass flux associated with the East Asian winter monsoon: Diversity and impacts. *Journal of Climate*, **1**, 1–37, https://doi.org/10.1175/JCLI-D-20-0319.1.

Lubis, S. W., and M. R. Respati, 2021: Impacts of convectively coupled equatorial waves on rainfall extremes in Java, Indonesia. *International Journal of Climatology*, **n/a**, https://doi.org/10.1002/joc.6967.

——, and Coauthors, 2022: Record-Breaking Precipitation in Indonesia's Capital of Jakarta in Early January 2020 Linked to the Northerly Surge, Equatorial Waves, and MJO. *Geophysical Research Letters*, **49**, e2022GL101513, https://doi.org/10.1029/2022GL101513.

——, S. Hagos, C.-C. Chang, K. Balaguru, and L. R. Leung, 2023: Cross-Equatorial Surges Boost MJO's Southward Detour Over the Maritime Continent. *Geophysical Research Letters*, **50**, e2023GL104770, https://doi.org/10.1029/2023GL104770.

Madden, R. A., and P. R. Julian, 1971: Detection of a 40–50 Day Oscillation in the Zonal Wind in the Tropical Pacific. *Journal of the Atmospheric Sciences*, **28**, 702–708, https://doi.org/10.1175/1520-0469(1971)028<0702:DOADOI>2.0.CO;2.

Matsuno, T., 1966: Quasi-Geostrophic Motions in the Equatorial Area. *Journal of the Meteorological Society of Japan. Ser. II*, **44**, 25–43, https://doi.org/10.2151/jmsj1965.44.1_25.

Maulana, M. T., T. Yamazaki, T. Iwasaki, and M. R. Abdillah, 2023: Regional variation of the influence of cross-equatorial northerly surge towards diurnal cycle of rainfall over Java Island. *Geoscience Letters*, **10**, https://doi.org/10.1186/s40562-023-00293-8.

Mori, S., and Coauthors, 2018: Meridional march of diurnal rainfall over Jakarta, Indonesia, observed with a C-band Doppler radar: an overview of the HARIMAU2010 campaign. *Progress in Earth and Planetary Science*, **5**, 47, https://doi.org/10.1186/s40645-018-0202-9.

Muhammad, F. R., S. W. Lubis, and S. Setiawan, 2021: Impacts of the Madden–Julian oscillation on precipitation extremes in Indonesia. *International Journal of Climatology*, **41**, 1970–1984, https://doi.org/10.1002/joc.6941.

Narulita, I., F. R. Fajary, M. R. Abdillah, M. R. Djuwansah, D. Sutjiningsih, E. Kusratmoko, and S. S. Moersidik, 2023: Synoptic conditions triggering extreme flood events in Bintan Island in early January 2021. *Meteorol Atmos Phys*, **135**, 45, https://doi.org/10.1007/s00703-023-00982-1.

Pang, B., R. Lu, A. A. Scaife, and R. Ren, 2023: Decadal change in cold surges over the South China Sea. *Journal of Climate*, **1**, https://doi.org/10.1175/JCLI-D-23-0254.1.

Peatman, S. C., A. J. Matthews, and D. P. Stevens, 2014: Propagation of the Madden-Julian Oscillation through the Maritime Continent and scale interaction with the diurnal cycle of precipitation: MJO Propagation and Scale Interaction with the Diurnal Cycle. *Q.J.R. Meteorol. Soc.*, **140**, 814–825, https://doi.org/10.1002/qj.2161.

Qian, J.-H., 2020: Mechanisms for the Dipolar Patterns of Rainfall Variability over Large Islands in the Maritime Continent Associated with the Madden–Julian Oscillation. *Journal of the Atmospheric Sciences*, **77**, 2257–2278, https://doi.org/10.1175/JAS-D-19-0091.1.

Ramage, C. S., 1971: *Monsoon Meteorology*. Academic Press,.

Riley, E. M., B. E. Mapes, and S. N. Tulich, 2011: Clouds Associated with the Madden–Julian Oscillation: A New Perspective from CloudSat. *Journal of the Atmospheric Sciences*, **68**, 3032–3051, https://doi.org/10.1175/JAS-D-11-030.1.

Saji, N. H., B. N. Goswami, P. N. Vinayachandran, and T. Yamagata, 1999: A dipole mode in the tropical Indian Ocean. *Nature*, **401**, 360–363, https://doi.org/10.1038/43854.

Satiadi, D., and Coauthors, 2023: Impacts of CENS and MJO phenomena on diurnal cycle of local convection, moisture convergence, and rainfall over land, coast, and sea areas in the western part of Java Island. *Meteorol Atmos Phys*, **135**, 42, https://doi.org/10.1007/s00703-023-00979-w.

Saufina, E., Trismidianto, Risyanto, I. Fathrio, and W. Harjupa, 2021: Impact of cross equatorial northerly surge (CENS) on Jakarta heavy rainfall and its interaction with tropical cyclone (Case study: 18-25 February 2020). *AIP Conference Proceedings*, **2366**, 050002, https://doi.org/10.1063/5.0059995.

Seow, M. X. C., M. E. E. Hassim, P. Venkatraman, and T. Tozuka, 2023: Atmospheric impacts of local sea surface temperatures versus remote drivers during strong South China Sea winter cold tongue events. *Quarterly Journal of the Royal Meteorological Society*, **149**, 556–572, https://doi.org/10.1002/qj.4423.

Shoji, T., Y. Kanno, T. Iwasaki, and K. Takaya, 2014: An Isentropic Analysis of the Temporal Evolution of East Asian Cold Air Outbreaks. *Journal of Climate*, **27**, 9337–9348, https://doi.org/10.1175/JCLI-D-14-00307.1.

Siswanto, G. J. van Oldenborgh, G. van der Schrier, G. Lenderink, and B. van den Hurk, 2015: Trends in High-Daily Precipitation Events in Jakarta and the Flooding of January 2014. *Bulletin of the American Meteorological Society*, **96**, S131–S135, https://doi.org/10.1175/BAMS-D-15-00128.1.

Stan, C., D. M. Straus, J. S. Frederiksen, H. Lin, E. D. Maloney, and C. Schumacher, 2017: Review of Tropical-Extratropical Teleconnections on Intraseasonal Time Scales: The Subseasonal to Seasonal (S2S) Teleconnection Sub-Project. *Rev. Geophys.*, **55**, 902–937, https://doi.org/10.1002/2016RG000538.

Suppiah, R., and X. Wu, 1998: Surges,cross-equatoriaflows and their links with the Australian summer monsoon circulation and rainfall. *Australian Meteorological Magazine*, **47**.

Trenberth, K. E., 1997: The Definition of El Niño. *Bulletin of the American Meteorological Society*, **78**, 7.

Trilaksono, N. J., S. Otsuka, and S. Yoden, 2012: A Time-Lagged Ensemble Simulation on the Modulation of Precipitation over West Java in January–February 2007. *Mon. Wea. Rev.*, **140**, 601–616, https://doi.org/10.1175/MWR-D-11-00094.1.

Trismidianto, and Coauthors, 2023: Interactions among Cold Surge, Cross-Equatorial Northerly Surge, and Borneo Vortex in influencing extreme rainfall during Madden–

Julian oscillation over the Indonesia Maritime Continent. *Meteorol Atmos Phys*, **135**, 43, https://doi.org/10.1007/s00703-023-00978-x.

Wati, T., T. W. Hadi, A. Sopaheluwakan, and L. M. Hutasoit, 2022: Statistics of the Performance of Gridded Precipitation Datasets in Indonesia. *Advances in Meteorology*, **2022**, e7995761, https://doi.org/10.1155/2022/7995761.

Wheeler, M., and G. N. Kiladis, 1999: Convectively Coupled Equatorial Waves: Analysis of Clouds and Temperature in the Wavenumber–Frequency Domain. *Journal of the Atmospheric Sciences*, **56**, 374–399, https://doi.org/10.1175/1520-0469(1999)056<0374:CCEWAO>2.0.CO;2.

Wheeler, M. C., and H. H. Hendon, 2004: An all-season real-time multivariate MJO index: Development of an index for monitoring and prediction. *Monthly Weather Review*, **132**, 1917–1932, https://doi.org/10.1175/1520-0493(2004)132<1917:AARMMI>2.0.CO;2.

Wu, P., M. Hara, H. Fudeyasu, M. D. Yamanaka, J. Matsumoto, F. Syamsudin, R. Sulistyowati, and Y. S. Djajadihardja, 2007: The Impact of Trans-equatorial Monsoon Flow on the Formation of Repeated Torrential Rains over Java Island. *SOLA*, **3**, 93–96, https://doi.org/10.2151/sola.2007-024.

——, A. A. Arbain, S. Mori, J. Hamada, M. Hattori, F. Syamsudin, and M. D. Yamanaka, 2013: The Effects of an Active Phase of the Madden-Julian Oscillation on the Extreme Precipitation Event over Western Java Island in January 2013. *SOLA*, **9**, 79–83, https://doi.org/10.2151/sola.2013-018.

Xavier, P., and Coauthors, 2020: Seasonal Dependence of Cold Surges and their Interaction with the Madden–Julian Oscillation over Southeast Asia. *Journal of Climate*, **33**, 2467–2482, https://doi.org/10.1175/JCLI-D-19-0048.1.

Yanai, M., and T. Maruyama, 1966: Stratospheric Wave Disturbances Propagating over the Equatorial Pacific. *Journal of the Meteorological Society of Japan. Ser. II*, **44**, 291–294, https://doi.org/10.2151/jmsj1965.44.5_291.

Yulihastin, E., T. Wahyu Hadi, N. Sari Ningsih, and M. Ridho Syahputra, 2020: Early morning peaks in the diurnal cycle of precipitation over the northern coast of West Java and possible influencing factors. *Ann. Geophys.*, **38**, 231–242, https://doi.org/10.5194/angeo-38-231-2020.

——, T. W. Hadi, M. R. Abdillah, I. R. Fauziah, and N. S. Ningsih, 2022: Propagation of Convective Systems Associated with Early Morning Precipitation and Different Northerly Background Winds over Western Java. *Journal of the Meteorological Society of Japan. Ser. II*, **100**, 99–113, https://doi.org/10.2151/jmsj.2022-005.

Zhang, C., 2005: Madden-Julian Oscillation. *Rev. Geophys.*, **43**, RG2003, https://doi.org/10.1029/2004RG000158.

Zhang, Y., K. R. Sperber, and J. S. Boyle, 1997: Climatology and Interannual Variation of the East Asian Winter Monsoon: Results from the 1979–95 NCEP/NCAR Reanalysis. *Monthly Weather Review*, **125**, 15.

Zhao, X., R. Lu, and J. Sun, 2023: Events of the Cross-Equatorial Flows Over the Maritime Continent During 1979–2020. *Journal of Climate*, **1**, 1–27, https://doi.org/10.1175/JCLI-D-22-0589.1.